Molecular Crystals and Liquid Crystals

ISSN: 1542-1406 (Print) 1563-5287 (Online) Journal homepage: https://www.tandfonline.com/loi/gmcl20

Synthesis and single crystal structure of a new polymorph of 5, 10, 15, 20-tetrakis-(4-chlorophenyl) porphyrin, H_2TTPCl_4: Spectroscopic investigation of aggregation of H_2TTPCl_4

Padma Dechan, Gauri Devi Bajju, Puneet Sood & Umar Ali Dar

To cite this article: Padma Dechan, Gauri Devi Bajju, Puneet Sood & Umar Ali Dar (2018) Synthesis and single crystal structure of a new polymorph of 5, 10, 15, 20-tetrakis-(4-chlorophenyl) porphyrin, H_2TTPCl_4: Spectroscopic investigation of aggregation of H_2TTPCl_4, Molecular Crystals and Liquid Crystals, 666:1, 79-93, DOI: 10.1080/15421406.2018.1512546

To link to this article: https://doi.org/10.1080/15421406.2018.1512546

MOLECULAR CRYSTALS AND LIQUID CRYSTALS
2018, VOL. 666, NO. 1, 99–113
https://doi.org/10.1080/15421406.2018.1512546

Taylor & Francis
Taylor & Francis Group

Synthesis and single crystal structure of a new polymorph of 5, 10, 15, 20-tetrakis-(4-chlorophenyl) porphyrin, H_2TTPCl_4: Spectroscopic investigation of aggregation of H_2TTPCl_4

Padma Dechan[a], Gauri Devi Bajju[a], Puneet Sood[b], and Umar Ali Dar[a]

[a]Postgraduate Department of Chemistry, University of Jammu, Jammu, India; [b]Advanced Materials Research Centre, Indian Institute of Technology, Mandi, Himachal Pradesh, India

ABSTRACT

5, 10, 15, 20-tetrakis-(4-chlorophenyl) porphyrin, H_2TTPCl_4, has been isolated as a new polymorph following the modified Adler's method and its X-ray crystal structure solved. The new polymorph (**I**) crystallises in the monoclinic space group, $P2_1/n$ with a = 10.1574(5) Å, b = 8.9827(4) Å, c = 20.9350(8) Å, $\beta = 102.532(4)^\circ$, V = 1864.62(15) Å^3, Z = 2. The previously found polymorph, prepared using Lindsay method was crystallised in monoclinic space group, $P2_1/a$ with a = 15.776 (13) Å, b = 8.646 (3) Å, c = 14.087 (5) Å, $\beta = 96.05$ (5)°, V = 1910.7 (3) Å^3, Z = 2. The main difference between the two polymorphs seems to be the different packing arrangement of molecules in their crystal lattices. The dramatic self aggregation property of new polymorph (**I**) has also been investigated. The investigation reveals that under certain conditions of solute concentration and pH of the media, the compound exhibits a strong tendency to exist in a prominent self aggregated state in head-to-tail type (j-aggregation) molecular alignment. The self association behaviour of (**I**) was confirmed by UV-Vis absorption spectra, performed in chloroform by varying concentrations and pH changes and ^{1}H NMR spectra, performed in deuterated chloroform at varying concentrations and their results have been discussed in detail.

Introduction

The synthesis and X-ray crystal structure of H_2TTPCl_4 belonging to monoclinic space group, $P2_1/a$, have been previously reported [1]. The compound was synthesized from p-chlorobenzaldehyde and pyrrole using Lindsay method. The structural data have discussed in detail the dihedral angles between the pyrrole and phenyl rings as well as average bond lengths and bond angles between various atoms. The crystal data have further shown that molecular structure of H_2TTPCl_4 was consequence of steric hinderances between the α-H atoms of the pyrrole and the ortho-H atoms of the phenyl rings. The packing diagram of the molecules along the [001] axes has also been shown. However, no further detail regarding the geometry of arrangement of molecules in the

CONTACT Gauri Devi Bajju gauribajju@gmail.com Postgraduate Department of Chemistry, University of Jammu, Jammu 180006, India.

unit cell and various inter and intramolecular forces that stabilises the crystal in its 3D crystal packing have been discussed. No further description of this complex has been published since, and, indeed, metal free porphyrin chemistry in general appears not to have been given adequate attention to date, especially if account is taken of the interesting aspects possibly associated with the packing of molecules. In an attempt to extend the present knowledge on H_2TTPCl_4, we recently reiterated the synthesis of H_2TTPCl_4 following modified Adler's method [2]. As a result we were able to isolate a new crystalline form of H_2TTPCl_4 belonging to monoclinic space group, $P2_1/n$. Single crystals of this compound have been obtained and their X-ray crystal structure has been elucidated.

Porphyrin are known to undergo strong self-aggregation in solutions [3–7] which enables them to exhibit diverse chemical and photophysical properties [8,9]. Porphyrins generally aggregate in a parallel manner (plane-to-plane stacking) to form a sandwich-type arrangement (H-aggregate) or in a head-to-tail arrangement (end-to-end stacking) to form a J-aggregate [10]. Among the various techniques available for studying aggregation in solution, UV-vis [11–14] and NMR [13–16] spectroscopies are most often used. This phenomenon of self aggregation in macrocylic porphyrin compounds has always attracted us and this led us to investigate whether or not the self aggregation property is exhibited by the new polymorph (**I**). Surprisingly, the compound exhibited prominent self aggregation under certain conditions in solutions as confirmed by UV-Visible and ^1H NMR spectroscopy. The Scheme 1 represents the structure of a mono-nuclear and j-aggregated H_2TTPCl_4.

Results and discussion

Preparation and crystallisation

Our procedure for the synthesis of solid monoclinic ($P2_1/n$) H_2TTPCl_4 (**I**) is different to that followed previously by Hokelek & Ulku for the monoclinic ($P2_1/a$) form. The previously reported polymorph was prepared from p-chlorobenzaldehyde and pyrrole by the Lindsey method using boron trifluoride etherate as catalyst. In ours method, we carried out the acid catalysed condensation reaction between equivalent moles of pyrrole and 4- chlorobenzaldehyde in the presence of propionic acid solution, followed by addition of ethylic ether (10 mL) following modified Adler's method [2] (Scheme 2). This method afforded us a new polymorph, which crystallized in the form of shiny violet crystals suitable for X-ray investigation. On completion of reaction, the needle shaped violet crystals were obtained after leaving the reaction mixture undisturbed at room temperature for about 10 days.

Single-crystal X-ray data collection and structure determination of (I)

The single crystal of the title compound (**I**) was examined under a microscope and a suitable crystal with dimension $0.28 \times 0.133 \times 0.107$ was selected for single-crystal X-ray crystallography. Single-crystal X-ray diffraction data were collected on a CCD Agilent SUPERNOVA E (Dual) diffractometer. The numerical details relating to the data

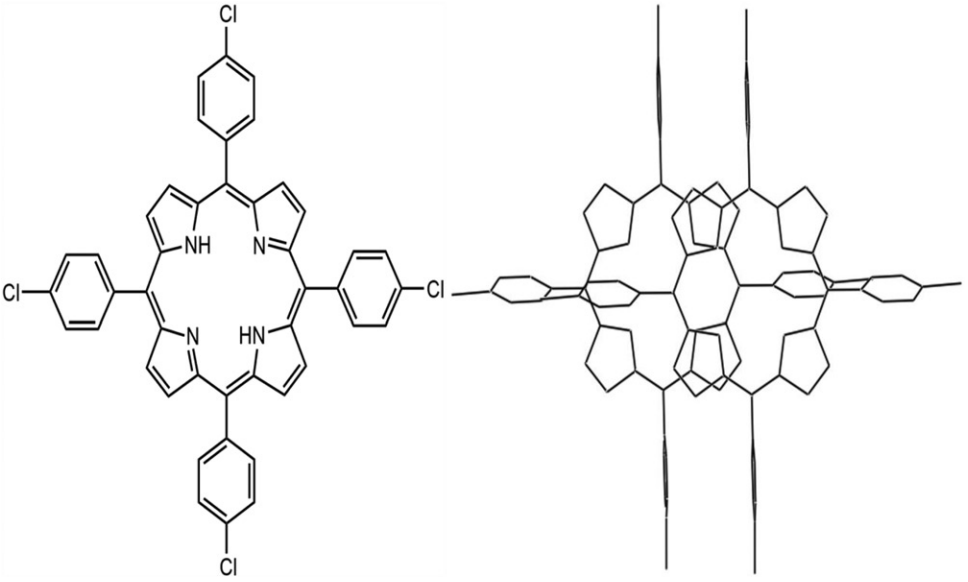

Scheme 1. (a) Structure of H_2TTPCl_4 monomer (b) Fragment of the structure of j-aggregated H_2TTPCl_4.

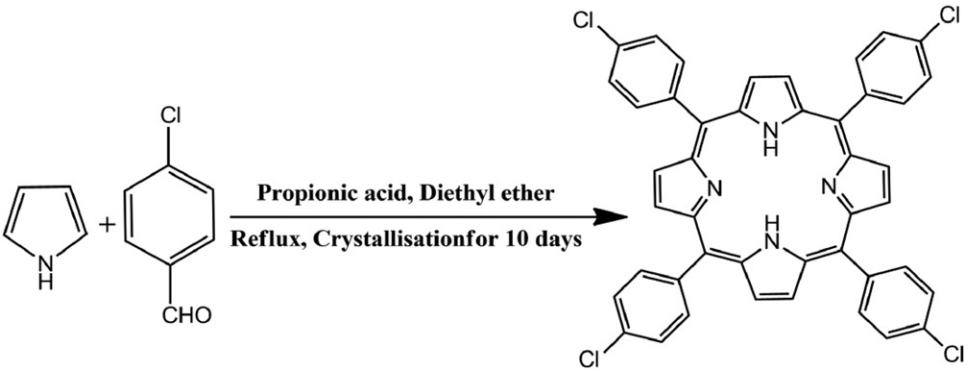

Scheme 2. Synthetic route for (**I**).

collection, data processing, and refinement of the X-ray structures of the compound are listed in Table 1 (CCDC number: 1860694).

Crystal structure and crystal packing diagrams of (I)

The Ortep representation of (**I**) along with the crystallographic labeling scheme is given in Fig. 1. As expected, the 24 atoms porphyrin core is nearly planar (dihedral angle, 5.01 Å), which shows a little but no significant distortion. On the contrary, the four phenyl rings are tilted from the N2/N4/N2/N4 porphyrin core planes by 66.38° (C15) and 88.67° (C23) showing significant out of porphyrin N4 core plane distortion [Fig. 2 (a)]. And as observed in the previous form [1], the driving force for the out of plane distortion of peripheral p-chloro phenyl rings seems to be the steric interaction between

Table 1. Numerical details of the solution and refinement of the crystal structures of (**I**).

Compound (**I**)	
Chemical formula	$C_{44}H_{26}Cl_4N_4$
Formula weight	752.49
Temperature/K	293 (2)
Crystal system	monoclinic
Space group	$P2_1/n$
a/Å	10.1574 (5)
b/Å	8.9827 (4)
c/Å	20.9350 (8)
α/°	90.00
β/°	102.532 (4)
γ/°	90.00
Volume/Å^3	1864.62 (15)
Z	2
ρ_{calc}g/cm^3	1.340
μ/mm^{-1}	3.178
F(000)	772.0
Crystal size/mm^3	0.28 × 0.133 × 0.107
Radiation	CuKα ($\lambda = 1.54184$)
2Θ range for data collection/°	9.02 to 133.56
Index ranges	$-12 \leq h \leq 11$, $-10 \leq k \leq 7$, $-24 \leq l \leq 23$
Reflections collected	5828
Independent reflections	3271 [$R_{int} = 0.0182$, $R_{sigma} = 0.0235$]
Data/restraints/parameters	3271/0/235
Goodness-of-fit on F^2	1.087
Final R indexes [I>=2σ (I)]	$R_1 = 0.0642$, $wR_2 = 0.1935$
Final R indexes [all data]	$R_1 = 0.0759$, $wR_2 = wR_2 = 0.2113$
Largest diff. peak/hole / e Å^{-3}	0.70/-0.64

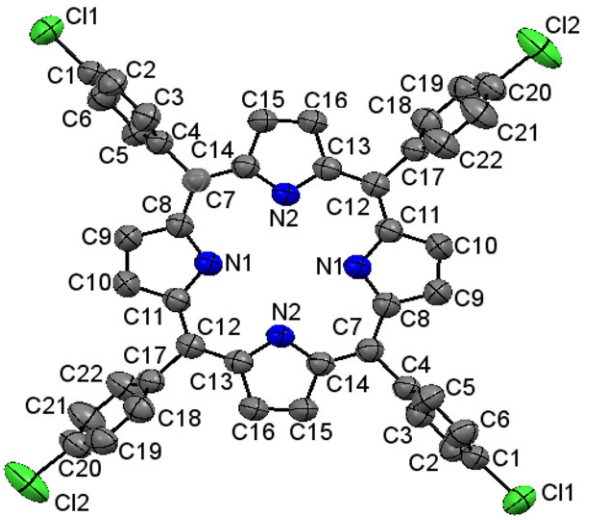

Figure 1. The ORTEP representation of the molecular structure with atom-labeling scheme for compound (**I**). Ellipsoids are shown at 50% probability level. Hydrogen atoms are omitted for clarity.

the neighbouring phenyl and pyrrole H atoms [H18 … H16 2.719 Å, H22 … H10 2.819 Å, H3 … H15 3.025, H9-H5 3.060 Å] and the close van der Waals contact between the pyrrole (N)H atoms [H2-H2 2.432 Å] [Fig. 2 (b)]. The inner NH groups of porphyrin core are involved in intramolecular bifurcated N— H···(N,N) hydrogen bonds as shown in Fig. 2 (b). Hydrogen bonds are listed in Table 2. The observed bond lengths and

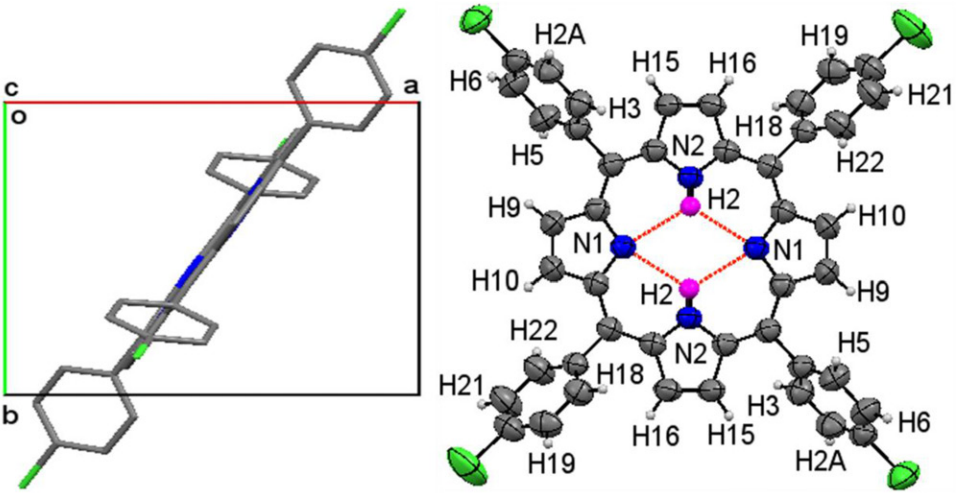

Figure 2. (a) Side view of compound (**I**) along c axes, showing the out of plane distortion of the peripheral p-chloro phenyl rings (b) ORTEP view of compound (**I**) showing the bifurcated N—H···(N,N) hydrogen bonds as red color dashed lines. The contact atoms are shown as blue (N) and pink (H) spheres.

Table 2. Hydrogen bonds for (**I**).

D—H … A	d(D-H)	d(H … A)	d(D … A)	< (DHA)
$N2^{i}$—H2···$N1^{i}$	0.861	2.364	2.903	121.01
$N2^{ii}$—H2···$N1^{i}$	0.861	2.364	2.923	120.53

Symmetry code: (i) x, y, z; (ii) 1 − x, 1 − y, 1 − z.

Table 3. Bond lengths (Å).

Cl1-C1	1.740 (3)	C12-C17	1.494 (4)
Cl2-C20	1.743 (4)	C17-C18	1.391 (5)
N1-C11	1.369 (4)	C17-C22	1.374 (5)
N1-C8	1.365 (4)	C4-C3	1.383 (5)
N2-C14	1.364 (4)	C4-C5	1.385 (5)
N2-C13	1.364 (4)	C9-C10	1.345 (5)
C14- C7	1.395 (4)	C15-C16	1.352 (5)
C14-C15	1.426 (4)	C3-C2	1.375 (5)
C13-C12	1.400 (4)	C2-C1	1.367 (6)
C13-C16	1.431 (4)	C1-C6	1.383 (6)
C7- C14	1.395 (4)	C18-C19	1.389 (5)
C7-C8	1.398 (4)	C5-C6	1.383 (5)
C7-C4	1.496 (4)	C19-C20	1.369 (6)
C11-C12	1.398 (4)	C22-C21	1.376 (5)
C11-C10	1.444 (4)	C20-C21	1.343 (6)
C8-C9	1.449 (4)		

bond angles (Tables 3 and 4) of the porphyrin macrocycle of present form are not significantly different from those of previous form.

The main difference between the present and previous form of H_2TTPCl_4 is very likely in the type of crystal packing. Fig. 3 shows the arrangement of the molecules of present form in the unit cell along the [001] axes. For comparison one can refer the packing arrangement of molecules in the unit cell of previous form [1] along the same axes. In the packing diagram representation of present form, each of the eight corners

Table 4. Bond angless (°).

C8-N1-C11	106.0 (2)	C22-C17-C18	118.2 (3)
C14-N2-C13	109.9 (2)	C3-C4-C7	121.0 (3)
N2-C14-C7	127.1 (3)	C3-C4-C5	118.3 (3)
N2-C14-C15	107.2 (3)	C5-C4-C7	120.7 (3)
C7-C14-C15	125.6 (3)	C10-C9-C8	106.8 (3)
N2-C13-C12	126.5 (3)	C16-C15-C14	107.9 (3)
N2-C13-C16	106.9 (3)	C15-C16-C13	108.0 (3)
C12-C13-C16	126.5 (3)	C9-C10-C11	107.0 (3)
C14-C7-C8	125.6 (3)	C2-C3-C4	121.5 (4)
C14-C7-C4	116.2 (3)	C1-C2-C3	119.0 (3)
C8-C7-C4	118.3 (3)	C2-C1-C11	119.4 (3)
N1-C11-C12	125.4 (3)	C2-C1-C6	121.5 (3)
N1-C11-C10	110.1 (3)	C6-C1-C11	119.1 (3)
C12-C11-C10	124.5 (3)	C19-C18-C17	120.3 (3)
N1-C8-C7	125.8 (3)	C6-C5-C4	121.3 (3)
N1-C8-C9	110.1 (3)	C20-C19-C18	119.0 (3)
C7-C8-C9	124.0 (3)	C5-C6-C1	118.5 (4)
C13-C12-C17	116.7 (3)	C17-C22-C21	121.3 (4)
C11-C12-C13	125.5 (3)	C19-C20-C12	119.1 (3)
C11-C12-C17	117.8 (3)	C21-C20-C12	119.4 (3)
C18-C17-C12	121.6 (3)	C21-C20-C19	121.5 (3)
C22-C17-C12	120.3 (3)	C20-C21-C22	119.7 (4)

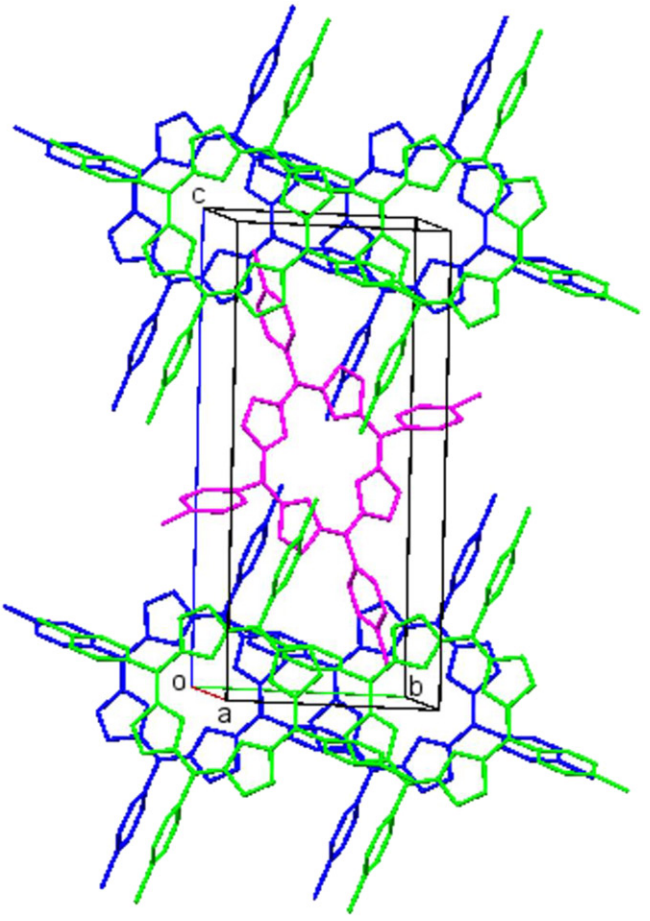

Figure 3. Packing of molecules of (**I**) along the [001] axes. Hydrogen atoms are omitted for clarity.

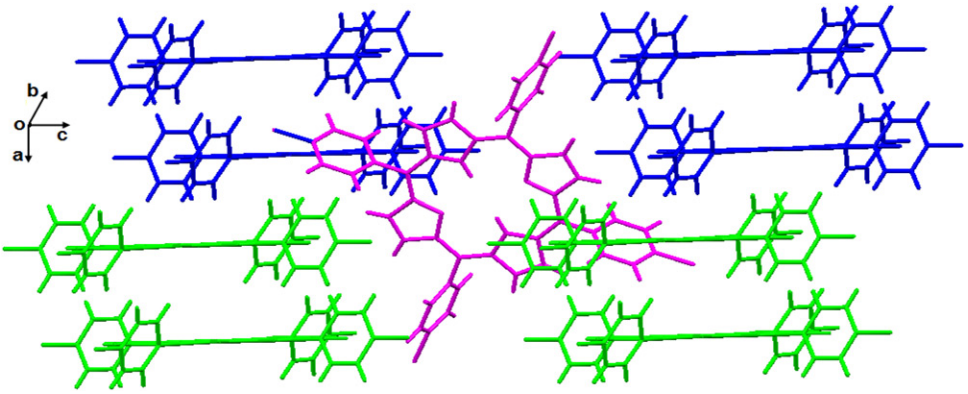

Figure 4. Formation of two sets of offset or slipped multilayer stacks (shown by blue and green colors) inter-linked by a single unstacked molecule (shown as pink) in (**I**).

as well as the body of the monoclinic unit cell is occupied by the H_2TTPCl_4 monomers (Fig. 3). The molecules at the corners are shown by blue and green colors while as the molecule in the body of unit cell is shown as pink for clarity. One can clearly observe from Fig. 3, that the molecules at the adjacent corners of the unit cell are stacked one above another in a slightly slipped manner (j-type alignment). Such type of stacking is not observed in the unit cell of previous polymorph along [001] axes [1]. In another packing diagram representation of present form (Fig. 4), two sets of offset or slipped multilayer stacks are formed by the corner occupied molecules that are bridged by a single body centre occupied molecule. In each set of multilayer stacks, four porphyrin molecules act remarkably as pairs forming two sets of dimeric pairs (a blue pair and a green pair). The two porphyrin units in each of the two dimeric pairs are stacked one above another in a j-type fashion through π–π interactions, with closest atom–atom distances of 3.51Å [Fig. 5 (a)]. The center-to-center and vertical distance between the two molecules of porphyrin pairs (blue pairs and green pairs) is measured to be 8.7-8.8 Å and 5.592 Å. In addition to π-π interactions, there are number of C–H$\cdots\pi$ (C … C 3.51–3.78 Å) interactions that bound the two molecules in dimeric pairs [Fig. 5 (b)]. The driving force is the enthalpy driven attractive interaction between π-systems leading to the stacks of molecules. Further, the two porphyrin pairs (blue pair and green pair) in each of the two set of multilayer stack are inter-connected by a two points C-H$\cdots\pi$ (C … C 3.51 Å) interactions (shown by black dashed lines) [Fig. 5(b)]. The driving force is the directional orientation of the C-H (donor) and C-C (acceptor) species of the interacting porphyrin molecules of each pair. The existence of C-H$\cdots\pi$ interactions resulted in greater degree of slippage of stacked layers. It is interesting to note that the H_2TTPCl_4 monomer in the body of unit cell (shown as pink) is not involved in the formation of stacked layers, however they interact with the molecules forming offset multilayers by three types of non covalent forces i.e π-π (C … C 3.51-3.58 Å), C–H$\cdots\pi$ (C … C 3.56–3.75 Å) weak C-H … Cl (H … Cl 3.28-3.29 Å) (Fig. 6).

Absorption spectroscopy

Fig. 7 depicts a typical monomeric (blue) and j-aggregated (olive green) absorption spectra of (**I**) in chloroform. The typical UV-vis spectra of porphyrins feature two

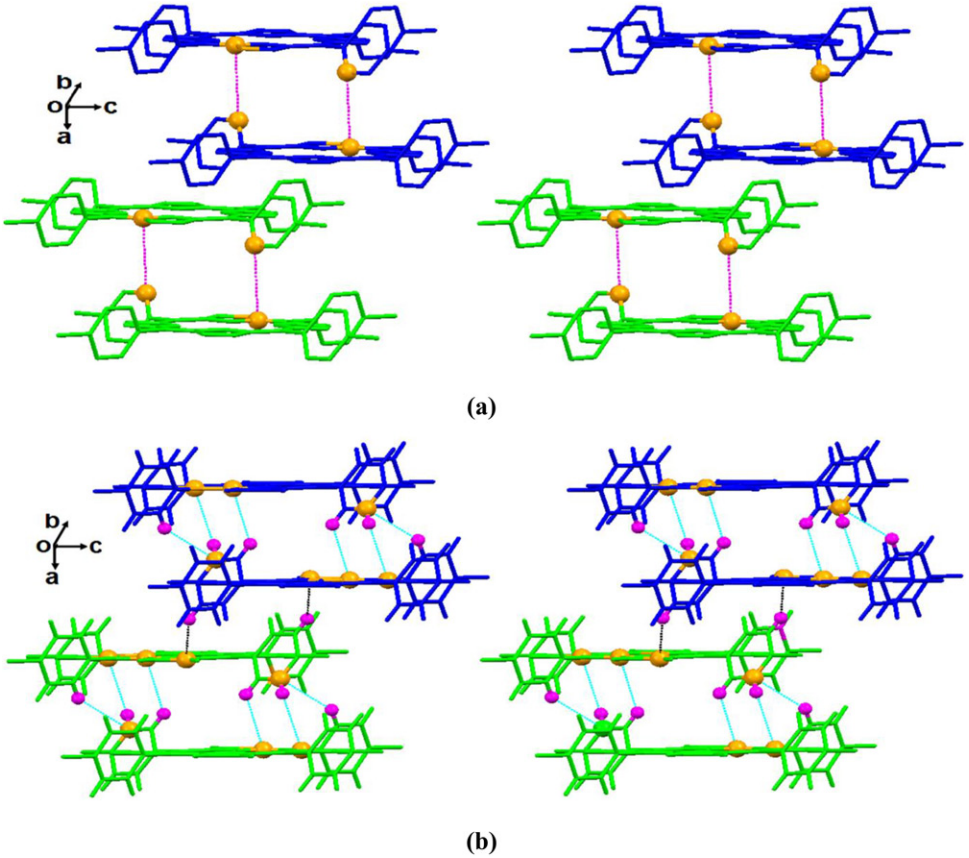

Figure 5. Offset or slipped face-to-face stacking geometry in the crystal lattice of (I) stabilised by $\pi\cdots\pi$ (a) and CH$\cdots\pi$ (b) interactions. The atoms involved in directional interactions are shown by orange (C) and pink (H) spheres. The molecule in the body of unit cell is omitted for clarity.

distinct absorption bands, namely B (or soret) band and Q-bands, that are attributed to $\pi-\pi^*$ transition within the highly conjugated porphyrin π-system. To confirm the aggregation of present form of H_2TTPCl_4 in pure chloroform, we measured the absorption spectra at two different concentrations at room temperature. The absorption spectrum of free base H_2TTPCl_4 measured at lower concentration i.e. $\sim$ 4.0 x 10^{-6}M exhibited an intense Soret band (B band) at 419 nm and four weak Q bands centered on 514, 550, 591 and 648 nm respectively (Fig. 7). The spectrum corresponded for non-aggregated monomeric complex, since no spectral change was observed with significant dilution of this solution. On measuring the spectra at slightly higher concentration $\sim 3.0 \times 10^{-3}$M, an intense and a narrow absorption B band that was red shifted from 419 to 422nm, also followed by very small red shift and increased absorbance of Q bands was observed. The red shift of absorption bands, especially B band is indicative of porphyrin self aggregation through head-to-tail molecular ordering [17,18].

On measuring the absorption spectra in acidic media (pH = 4), a split soret bands appeared [Fig. 8 (a)]. The splitting of the Soret band into two individual Lorentzian bands located around 420 and 448nm respectively was the result of a tendency to form

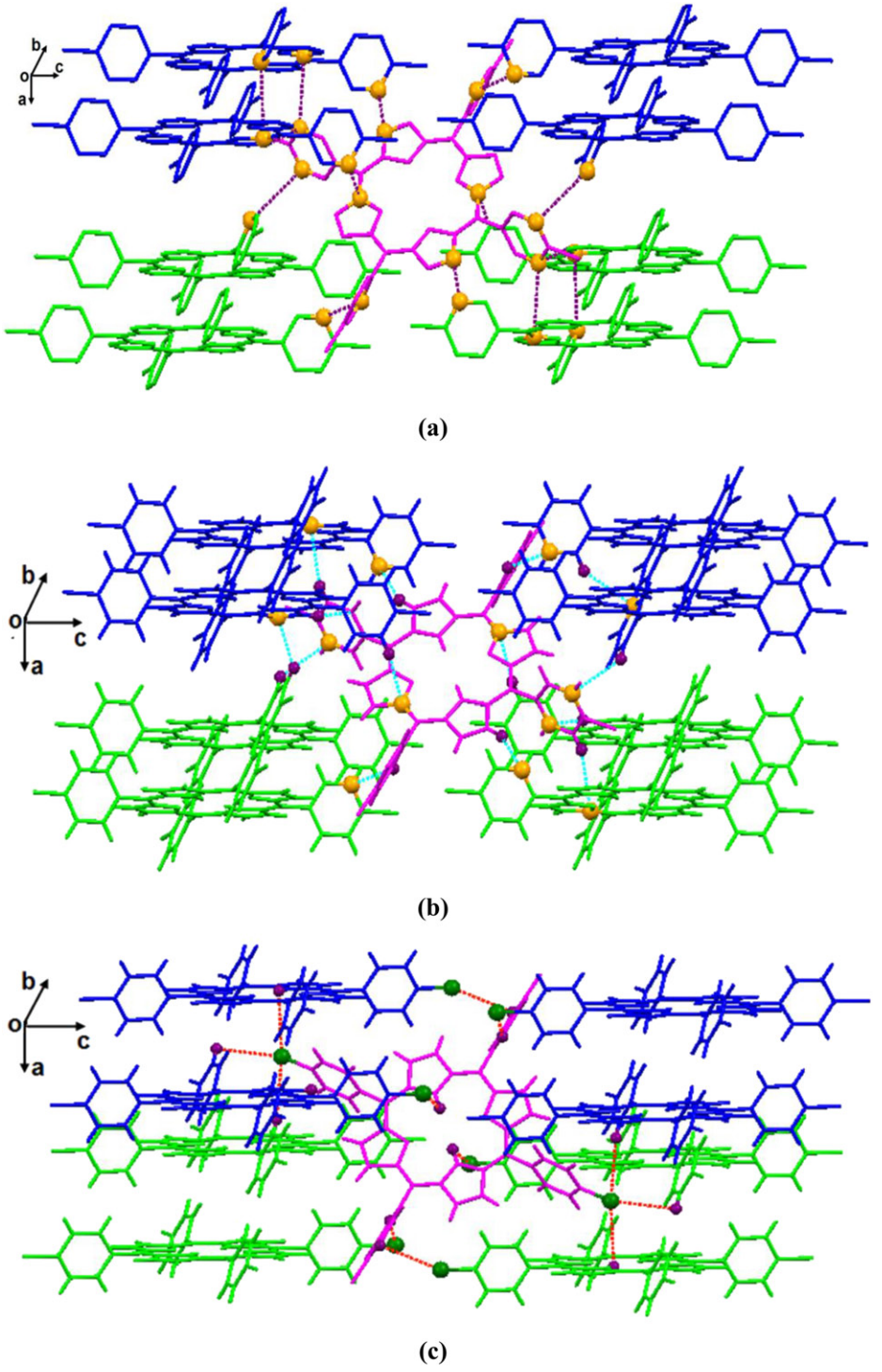

Figure 6. Directional interaction of H_2TTPCl_4 monomer lying in the body of unit cell (shown as pink) with neighbouring monomers (shown as blue and green) occupying each of eight corners of the unit cell of (**I**) by ($\pi\cdots\pi$) (a), (C-H$\cdots\pi$) (b) and (C-H$\cdots$Cl) (c) hydrogen bonding interactions. The contact atoms are shown as orange (C), purple (H) and dark green (Cl) spheres.

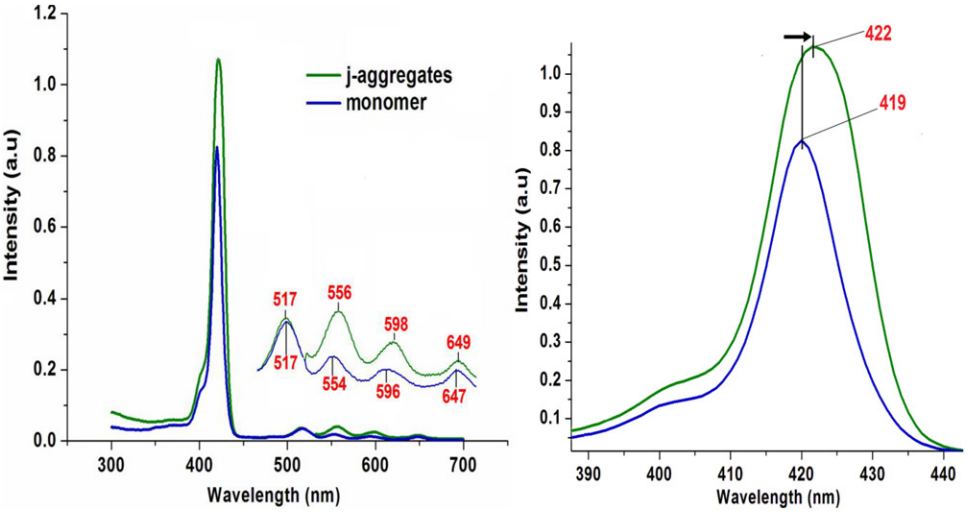

Figure 7. (a) The UV/Vis absorption spectra of monomeric (blue, 4.0 x 10^{-6}M) and j-aggregated H_2TTPCl_4 (**I**) (olive green, 3.0×10^{-3}M) in $CHCl_3$ at room temperature (b) enlargement of soret band regions (arrow signifies shift in the monomer B band towards higher wavelength).

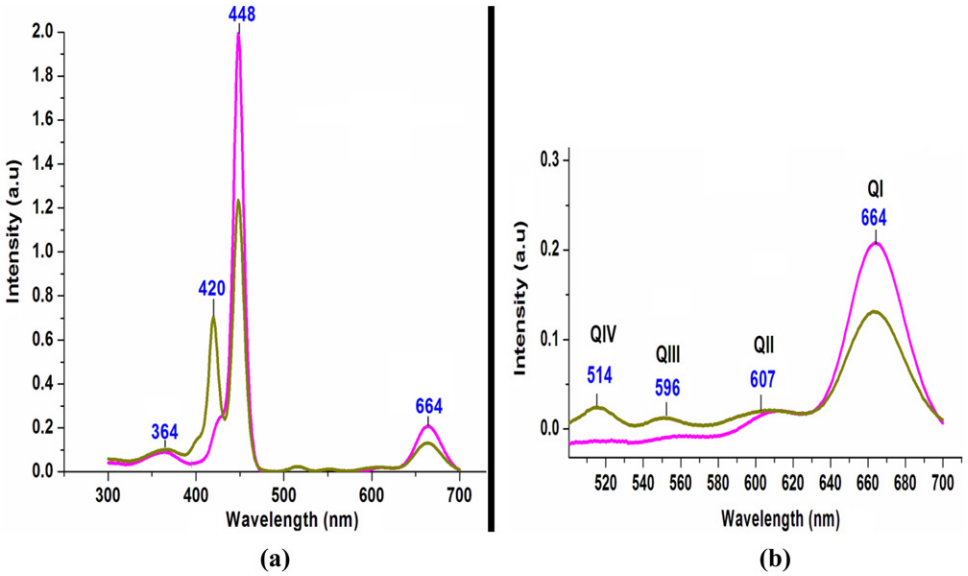

Figure 8. (a) The UV/Vis absorption spectra of H_2TTPCl_4 (**I**) in $CHCl_3$ at pH = 4 (green) and pH = 3 (magneta) (b) enlargement of Q band regions.

aggregates. Here the bands centered around 420 and 448nm are attributed to the monomeric and that of aggregated H_2TTPCl_4. In the acidic media the addition of protons to the nitrogen atoms in the center of porphyrin ring induces the partial positive charge (Fig. 9) in the central part of the molecule [19]. The dication generations leds to gradual decrease of the monomer absorption B band at 420nm and appearance of sharp and narrow red shifted band (known as j-band) at 448nm. This was also followed by increase in the intensity of Q I band, which is forbidden otherwise. The red shift of the Soret band

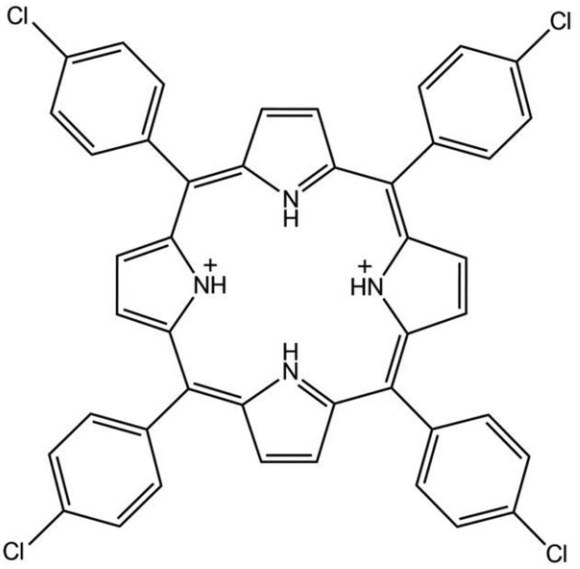

Figure 9. Structure of the H_2TTPCl_4 (I) porphyrin dication ($H_2TTPCl_4^{2+}$) at pH = 4 and lower.

is attributed to a side-by-side aggregation and a formation of J-aggregates. At pH = 3, the monomer absorption B band diminished completely [Fig. 8 (a)]. and a high intensity j-band appeared. Also the QII, QIII, QIV bands were almost nearly diminished leaving behind the high intensity QI band [Fig. 8 (b)]. The QI band was bathochromic shifted from 647 to 664nm. Therefore in the high ionic strength media, the Q bands were reduced to only one, red shifted towards 664nm accompanied by significant increase in intensity. The decrease in the number of Q bands was attributed to increase in the symmetry (D2h to D4h) of the porphyrin by protonation, and generation of the dication species [19]. It can be noted from Fig. 8 (a) that in the high ionic strength media, H_2TTPCl_4 exhibited the spectra of hyper p-type. In addition to the Soret band around 400 nm, there appeared an extra absorption band at λmax ~364 nm. The extra band at 364nm may be attributed to the charge transfer transitions from the lone pair p orbitals of the peripheral chlorine atoms to empty π^* orbitals of porphyrin.

^{1}H NMR spectroscopy

The self aggregation of H_2TTPCl_4 (**I**) was also studied by ^{1}H NMR spectroscopy, and the results showed that aggregation occurs at high molar concentration. The ^{1}H NMR spectra of a typical monomeric (blue) and self aggregated (olive green) H_2TTPCl_4 in deuterated chloroform is shown in Fig. 10 (a). While selected regions of the spectra are given in Fig. 10 (b). At low solute concentration i.e. ~ 5 X 10^{-5} M, notably sharp resonance signals appeared at δ 8.87(s), 8.17-8.15(d), 7.79-7.77(d) and -2.84(s) for ortho (Hc), meta (Hb), beta (Ha) and amino pyrrole protons (Hd). The spectrum corresponded for non- aggregated monomeric complex, since no change in the position as well as shape of resonance peaks were observed on dilution of the solution. However at higher concentration ~ 5 X 10^{-3} M, the intensities of mononuclear resonance signals fell off drastically and a broader upfielded peaks appeared. The decrease in the intensity

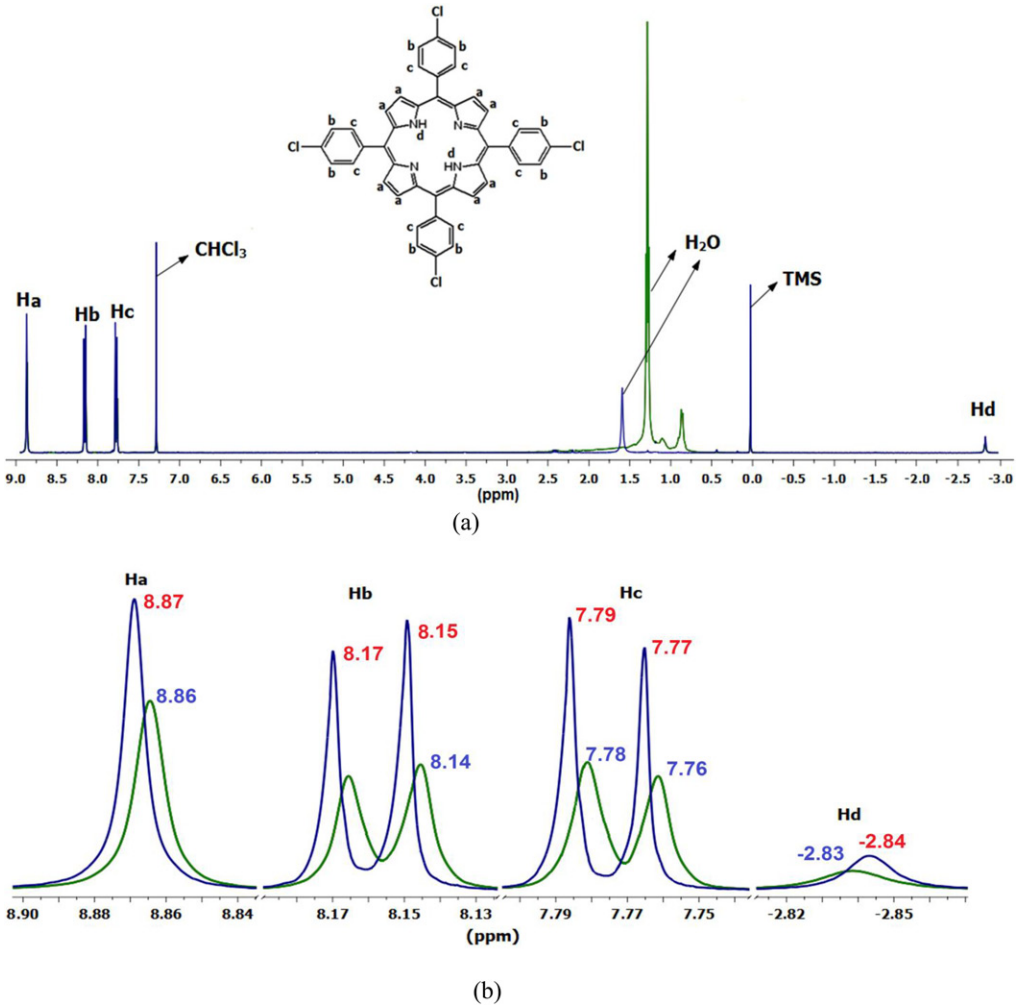

Figure 10. (a) ^{1}Hmr spectra (400 MHz pulse FT) of monomeric (blue, 5 X 10^{-5} M) and j-aggregated (olive green, 5 X 10^{-3} M) H_2TTPCl_4 (**I**) in $CDCl_3$. Extra peaks at δ 7.2 p.p.m and 1.5-1.6 p.p.m is due to presence of undeuterated chloroform and water molecules (b) Magnified view of ortho, meta, beta and amino pyrrole proton signals.

followed by slight broadening of resonance signal at $\sim$ 5 X 10^{-3} M signified that aggregation had already set at this concentration [20]. The shifting of resonance signals was due to the additional magnetic field generated by the ring current of another macrocycle lying in close proximity in aggregated condition [21]. The higher tendency of the H_2TTPCl_4 (**I**) to aggregate in chloroform presumably reflects the lower solvating power of chloroform for this compound. Because the ^{1}H NMR spectrum of H_2TTPCl_4 sharpened up at concentrations around 10^{-5}M and lower, this concentration can be roughly considered as the critical aggregation concentration in this solvent.

Conclusion

In summary, we have reported the single crystal molecular structure of second polymorph of H_2TTPCl_4 which crystallizes in the monoclinic space group, $P2_1/n$. In its

crystal structure, each of the eight corners as well as the body of monoclinic unit cell is occupied by H_2TTPCl_4 monomers. The molecules occupying the corners of the unit cell formed two sets of offset or slipped (j-type) multilayer stacks that are interlinked by a H_2TTPCl_4 molecule lying in the body centre of unit cell by three types of non covalent forces i.e. $\pi\cdots\pi$, C-H$\cdots\pi$ and weak intermolecular C-H$\cdots$Cl interactions. In each set of multilayer stacks, four porphyrin molecules form two sets of dimeric pairs. The two molecules in each dimeric pairs are bound together by various $\pi\cdots\pi$ and C-H$\cdots\pi$ interactions and two dimeric pairs are interlinked by a two point C-H$\cdots\pi$ interactions. The analysis of the optical absorption spectra of H_2TTPCl_4 in pure chloroform solution indicated that at low concentration $\sim 10^{-6}$M, the molecules exists as simple monomers, however at higher concentration $\sim 10^{-3}$M, they tend to aggregate in a head to tail manner (j-aggregation). The most important feature observed in the acidic media at pH = 4, was the appearance of low intensity monomer B band and a sharp high intensity j-band. As the ionic strength of the media increases at pH = 3, the monomer B band completely disappeared leaving behind a narrow energetic j-band and an intense QI band. The concentration dependent ^{1}H NMR spectra of H_2TTPCl_4 revealed that the compound exists as discrete monomers at concentration $\sim 10^{-5}$ M and lower. Above this concentration, the compound exhibited dramatic self aggregation leading to significant quenching and broadening of resonance signals.

Experimental

Chemicals

The analytical grades chemicals were used for the synthesis of free base H_2TTPCl_4 (**I**). Pyrrole, 4-chlorobenzaldehyde, propionic acid and diethylether were purchased from sigma Aldrich and were used as received.

Meaurements

UV-Visible spectra were obtained on PG spectrophotometer; model T-90. ^{1}H NMR spectra were recorded on Bruker spectrometer, model AV 400 N (400 MHZ), using $CDCl_3$ as solvent and TMS as internal reference.

Synthesis

The new polymorph of H_2TTPCl_4 was synthesized following modified Adler's acid catalysed condensation method [2] as shown in Scheme 2. To the boiling solution of propionic acid (50mL) containing 0.05 moles of 4-chlorobenzaldehyde, fitted with a water condensor, 0.05 moles of pyrrole was added dropwise with vigorous stirring. The mixture was allowed to reflux for 30-40 min, followed by addition of small amount (10mL) of ethylic ether to cause rapid crystallisation. The reaction was monitored by TLC in a dichloromethane/n-hexane (30:70 v/v) system. After completion of the reaction, the reaction mixture was allowed to cool at room temperature and then left undisturbed for about 10 days. A needle shaped shine violet crystals of (**I**) were obtained in 65% yield.

Solution and refinement of the crystal structure of compound (I)

Reflection data were measured at 293(2) K. The crystal was mounted under paratone oil and to get relative intensity data, the single crystal analysis was collected on a CCD Agilent SUPERNOVA E (Dual) diffractometer using monochromated Cu-Kα radiation ($\lambda = 0.154184$ Å) at 293(2) K. Using Olex2 [22], the structure was solved with the ShelXS [23] structure solution program using Direct Methods and refined with the ShelXL [23] refinement package using Least Squares minimisation. The positions of all the atoms were obtained by direct method. All non hydrogen atoms were refined anisotropically. The remaining H- atoms were refined with isotropic temperature factors, 1.2 U_{eq} of their parent atoms. Crystallographic data (cif) has been deposited with the Cambridge Structural Data Centre (CCDC) with reference number- 1860694.

Acknowledgment

This research was supported by CSIR (Council of Scientific and Industrial Research) India (grant No. 09/100(0190)/2016-EMR-I).

ORCID

Padma Dechan http://orcid.org/0000-0003-2783-4884
Gauri Devi Bajju http://orcid.org/0000-0002-6143-8853

References

[1] Hokelek, T., & Ulku, D. (1993). *Acta Cryst. C49*, 1667–1670.
[2] Adler, A. D., Longo, F. R., Finarelli, J. D., Goldmacher, J., Assour, J. & Korsakoff, L. (1967). *J. Org. Chem. 32*, 476–476.
[3] Akins, D. L., Zhu, H. R., & Guo. C. (1996). *J. Phys. Chem. 100*, 5420–5425.
[4] Andrade, S. M., Teixeira, R., Costa, S. M. B., & Sobral, A. J. F. N. (2008). *Biophys. Chem. 133*, 1–10.
[5] Pandey, R. K., Chitgupi, U., & Lakshminarayanan, V. (2012). *J. Porphyr. Phthalocyanines. 16*, 1055–1058.
[6] Ion, R. M., Grigorescu, M., Scarlat, F., Niculescu, V. I. R., Scarlat, F. L., & Gunaydin, K. (2001). *Rom Rep Phys. 53*, 281–292.
[7] Shirakawa, M., Nakata, K., Suzuki, M., Kobayashi, T., & Tokunaga, E. (2017). *J. Phys. Soc. Jpn. 86*, 044703.
[8] Mobius, D. (1995). *Adv.Materials. 7*, 437–444.
[9] Taguchi, T., Hirayama, S., & Okamoto, M. (1994). *Chem. Phys. Lett. 231*, 561–568.
[10] Giri, N. K., Banerjee, A., Scott, R. W. J., Paige, M. F., & Steer, R. P. (2014). *Phys.Chem.Chem.Phys. 16*, 26252–26260.
[11] Fox, J. M., Katz, T. J., Elshocht, S. V., Verbiest, T., Kauranen, M., Persoons, A., Thongpanchang, T., Krauss, T., & Brus, L. (1999). *J. Am. Chem. Soc. 121*, 3453–3459.
[12] Ishikawa, N., Ohno, O., Kaizu, Y., & Kobayashi, H. (1992). *J. Phys. Chem. 96*, 8832–8839.
[13] Cammidge, A. N, Cook, M. J., Harrison, K. J., & Mckeown, N. B. (1991). *J. Chem. Soc. Perkin Trans. 1. 12*, 3053–3058.
[14] Law, W. F., Liu, K. M., & Ng, D. K. P. (1997). *J. Mater. Chem. 7*, 2063–2067.
[15] Piechocki, C., & Simon, J. (1985). *J. Chem. Soc. Chem. Commun.* 259–260.

[16] Marcuccio, S. M, Svirskaya, P. I, Greenberg, S., Lever, A. B. P., Leznoff, C. C., & Tomer, K. B. (1985). *Can. J. Chem. 63*, 3057–3069.
[17] Snitka, V., Rackaitis, M., & Rodaite, R. (2005). *Sensors and Atuators B. 109*, 159–166.
[18] Eisfeld, A. & Briggs, J. S. (2006). *Chem. Phys. 324*, 376–384.
[19] Fagadar-Cosma, E., Enache, C., Tudose, R., Armeanu, I., Mosoarca, E., Vlascici, D., & Costisor. O. (2007). *Rev. Chim. (Bucuresti). 58*, 451–455.
[20] Abraham, R. J., Eivazi, F., Pearson, H. & Smith, K. M. (1977). *Tetrahedron. 33*, 2277–2285.
[21] Chen, M. J., & Rathke, J. W. (2001). *J. Porphyr.Phthalocyanines. 5*, 528–536.
[22] Dolomanov, O. V., Bourhis, L. J., Gildea, R. J., Howard, J. A. K., & Puschmann, H. (2009), *J. Appl. Cryst. 42*, 339–341.
[23] Sheldrick, G. M. (2008). *Acta Cryst. A64*, 112–122.